

# **Temperatures of Subduction Mélanges: Raman Thermometry of the Franciscan Complex**

William Lawrence

Advisor: Mark Brandon

Second Reader: Jay Ague

A Senior Thesis presented to the faculty of the Department of Geology and Geophysics,  
Yale University, in partial fulfillment of the Bachelor's Degree.

In presenting this thesis in partial fulfillment of the Bachelor's Degree from the Department of Geology and Geophysics, Yale University, I agree that the department may make copies or post it on the departmental website so that others may better understand the undergraduate research of the department. I further agree that extensive copying of this thesis is allowable only for scholarly purposes. It is understood, however, that any copying or publication of this thesis for commercial purposes or financial gain is not allowed without my written consent.

Will Lawrence, May 5<sup>th</sup>, 2022

**Abstract.** Subduction zone mélanges carrying exotic blocks have sparked decades of debate regarding their origins. Mud matrix mélanges that host high-grade blocks, including eclogites, in the Franciscan Complex, California have been proposed to derive from tectonic mixing within a subduction channel corner flow, or sedimentary mixing by submarine debris flows. Previous observations of large differences in metamorphic grade between mélange matrix and high-grade blocks are examined by Raman spectroscopy of carbonaceous material (RSCM) thermometry. A novel RSCM method is developed utilizing partial least squares (PLS) regression on a calibration dataset of 37 samples with well-defined metamorphic temperatures from the Alps and the Apennines. The resultant 6-component PLS model has a standard error of  $\pm 17$  °C and  $R^2 = 0.97$ .

The RSCM-PLS method is used to determine maximum metamorphic temperatures of mélange matrix and sandstone samples from six localities across the Franciscan (North Shell Beach, Goat Rock, Mount Diablo, Sunol Regional Wilderness, Diablo Range, and San Simeon). Matrix temperatures span 190 – 238 °C and are markedly low compared to those of enclosed high-grade blocks (~300 – 630 °C). With these temperatures the matrix could only have reached depths of 13 – 20 km, which is difficult to reconcile with tectonic exhumation of high-grade blocks, especially eclogites, from >50 km in a subduction channel. Furthermore, the thermal histories of CM grains in mud matrix are remarkably consistent compared to heterogeneous thermal histories observed for CM grains in Franciscan sandstones. These observations suggest a sedimentary origin for these mélanges as submarine debris flows, where suspended mud collected CM as it settled through the water column. Subsequent burial by subduction-accretion accounts for the uniform thermal histories and low metamorphic temperatures observed. Conversely, the sandstones acquired detrital CM grains with diverse thermal histories by traction during transport from the continental margin.

Two samples of serpentinite-mud mélange matrix, apparently enclosed within larger siliciclastic mélange bodies in the North Shell Beach-Goat Rock area, had anomalously high maximum metamorphic temperatures of ~387 °C. Their distinct petrography and thermal history indicate that they do not share a genetic relationship with the surrounding mélange, in which they appear to have been incorporated. One sample is associated with a selvage adjacent to a ~60 m garnet-amphibolite block and may represent a primary matrix that originally enclosed the block. It is speculated that these serpentinite-mud mélanges were shed from deeply originating diapirs as has been suggested for other detrital serpentinite deposits around the Franciscan.

## 1. Introduction

Regional-scale, chaotic bodies of rock containing blocks of various sizes in a variably deformed matrix of mud or serpentinite are found in subduction zone accretionary wedges worldwide. Since their discovery, these units have been termed *mélange*, a moniker that has been used by some researchers in a genetic sense indicating formation by tectonism (e.g. Hsü, 1968; Sengör, 2003) and by others in a descriptive sense referring to the presence of blocks in a finer matrix (e.g. Silver and Beutner, 1980; Wakabayashi, 2015). This divide is largely the result of ongoing controversy surrounding the processes responsible for the genesis of *mélanges*. Of special interest are so-called ‘exotic blocks’ that appear to have a genetic history separate from that of the surrounding matrix. These extraformational components were evidently introduced into the *mélange* and have ages and/or metamorphic grades that are distinct from the matrix. Several models have been put forth to explain the introduction of exotic blocks, and the genesis of *mélanges*. The three most popular proposals are 1) tectonically formed by return flow within a subduction channel corner flow, with blocks plucked from various levels in the subduction zone (Cloos, 1982; Shreve and Cloos, 1986; Cloos and Shreve, 1988a, 1988b), 2) sedimentary origin as mass-wasting deposits (olistostromes) in the trench, with blocks emplaced down-slope in debris flows (Aalto, 1981; Cowan, 1985; Wakabayashi, 2015), and 3) diapiric intrusion of mud/serpentinite, with blocks derived from the wall rock of the diapir (Brown and Westbrook, 1988; Orange, 1990; Tsujimori et al., 2007).

Along the California Coast Ranges, the Franciscan Complex is the prototypical example of a subduction complex and provides a >150 Myr history of continuous subduction (e.g. Wakabayashi, 2015). Of particular note is its mode of preservation, as its termination as a transform margin in the form of the San Andreas fault prevented the destruction of primary features of the accretionary wedge by orogenic collision. *Mélange* bodies of both siliciclastic and serpentinite matrix are especially characteristic of the Franciscan and carry a variety of exotic blocks including high-grade eclogites, amphibolites, and coarse blueschists (Coleman and Lanphere, 1971).

It has long been recognized that the enigmatic high-grade blocks in the Franciscan, appear out of ‘metamorphic equilibrium’ with the low-grade matrix in which they are enclosed (Bostick, 1974; Cloos, 1983). Cloos (1983) emphasized that the metamorphic contrast between high-grade blocks and shale matrix was sometimes primarily a result of a difference in

temperature rather than pressure. Thus, eclogites, amphibolites, and coarse blueschists metamorphosed at pressures of 7 to 10 kb (0.7 – 1.0 GPa, 25 – 35 km depth) could have been tectonically transported by mélangé matrix in the subduction channel without significant thermal metamorphism due to the depressed geothermal gradient. However, it has more recently been shown that Franciscan eclogite blocks formed under metamorphic pressures of ~1.6 – 2.5 GPa (Tsuji-mori et al., 2006; Page et al., 2007) corresponding to depths of ~50 – 80 km assuming a density of 3200 kg/m<sup>3</sup> and a lithostatic gradient. Additionally, more detailed field and petrographic studies at well-exposed mélangé bodies with visible block-matrix contacts have led to a growing recognition of the sedimentary origin of many mélanges (e.g. Cowan, 1985; Platt, 2015; Wakabayashi, 2015; 2021b; Krohe, 2017).

This paper aims to revisit the issue of the metamorphic discrepancy between high-grade blocks and enclosing matrix in the Franciscan mélanges. We present a new technique involving Raman spectroscopy of carbonaceous material (RSCM) which builds upon previous Raman thermometry methods by utilizing partial least squares (PLS) regression on a set of calibration spectra with known maximum metamorphic temperatures derived from the central and western Alps reference series of Lünsdorf et al. (2017) and vitrinite samples from the Suviana 1 well (Anelli et al., 1994). This method is used to provide a new and independent measurement of maximum metamorphic temperatures for matrix in a reconnaissance study of mélangé bodies across different localities in the Central belt of the Franciscan. The results are then discussed in the context of new observations regarding competing models for the genesis of subduction mélanges and the exhumation of high-grade rocks.

## **2. Geological Setting of the Franciscan Complex**

The Franciscan Complex is an accretionary wedge that formed from E-dipping subduction of the Farallon plate beneath North America from ca. 175 – 12 Ma, with accretion of most of the exposed rocks occurring between ca. 120 – 32 Ma (e.g. Wakabayashi and Dumitru, 2007; Wakabayashi, 2015; Mulcahy et al., 2018). Historically, the Franciscan has been divided into three subparallel NW-SE trending belts called the Coastal, Central, and Eastern belts (Berkland et al., 1972) (Figure 1). The Coastal belt is primarily characterized by zeolite grade sandstone and shale, the Central belt by shale and sandstone matrix mélangé hosting a variety of

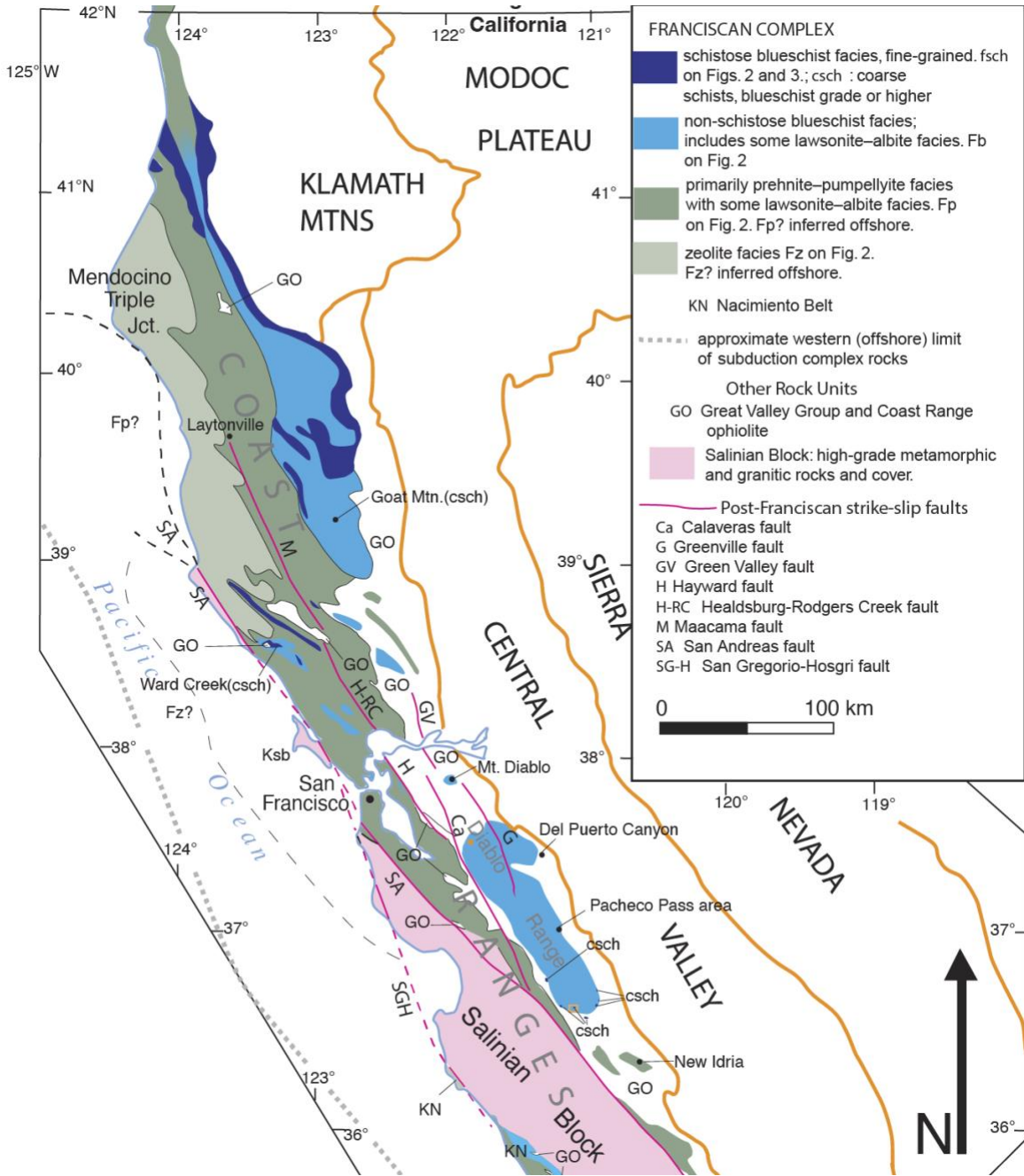


Figure 1. Geologic map of the Franciscan Complex. In the framework of the traditional belt nomenclature, the Eastern belt is shaded in blue and dark blue, the Central belt in green, and the Coastal belt in light green. San Simeon is located just south of the map area in Central belt rocks west of the Salinian Block. Adapted from Wakabayashi, 2015.

blocks, including those of high metamorphic grade, with zones of coherent sandstone and shale, and the Eastern belt by fault-bounded thrust sheets of coherent blueschist facies metasedimentary rocks and minor metavolcanics (e.g. Berkland et al., 1972; Blake et al., 1988). However, along-

strike variation in the Franciscan has been recognized to result in confusion regarding the correlation of units that have undergone contemporaneous accretion in the framework of the belt nomenclature (e.g. Wakabayashi, 2011).

The Coast Range Ophiolite (CRO) structurally overlies the Franciscan, from which it is separated by the Coast Range fault. The CRO has undergone seafloor hydrothermal metamorphism from zeolite to greenschist or higher grade, but burial metamorphism of only zeolite-grade (Evarts and Schiffman, 1983), and is composed of serpentinite ultramafic rocks, gabbro, basalt, and other plutonic and volcanic rocks (e.g. Hopson et al., 1981; 2008). Overlying the CRO are the sedimentary rocks of the Great Valley Group (GVG) which include sandstones, shales, and conglomerates. This forearc sedimentary sequence has only undergone zeolite facies metamorphism near its base (Dickinson et al., 1969), and is more or less contemporaneous with the deposition of Franciscan clastic sedimentary rocks (e.g. Dickinson, 1970; Dumitru et al., 2015). Notably, the basal GVG has shale and serpentinite olistostrome horizons that host high-grade blocks equivalent to those found in the Franciscan mélanges (e.g. Hitz and Wakabayashi, 2012). The Sierra Nevada batholith, the eroded remnant of the magmatic arc associated with the Franciscan subduction system, lies inboard of the GVG. The three larger lithotectonic belts of the Franciscan, CRO-GVG, and Sierra Nevada batholith correspond to the accretionary wedge, forearc basin, and magmatic arc of a single subduction system (Figure 1).

The Franciscan is dominated by siliciclastic sedimentary rocks representing off-scraped and underplated trench-fill sediments (Dickinson, 1970) with comparatively minor occurrences of basalt, chert, limestone, and serpentinite. Typical Franciscan units are rich in clastic sedimentary rocks, including siliciclastic mélange horizons, as those seen in the sea cliff exposures of San Simeon and Shell Beach, and at inland exposures like those in the Sunol Regional Wilderness (e.g. Platt, 2015; Wakabayashi, 2015; 2021b). Other localities have high proportions of basalt and chert, in many places present as coherent ‘ocean-plate stratigraphy’ (OPS), as is seen at Mt. Diablo (Wakabayashi, 2021a). The volcanic rocks of the Franciscan are remnants of accreted material from the upper horizons of the subducting oceanic plate (e.g. Wakabayashi, 2015). Olistostrome blocks displaced from the upper plate or from earlier accreted and exhumed Franciscan material also account for some siliciclastic, pelagic, volcanic and plutonic rocks (e.g. Aalto, 1989; Erickson, 2011; Wakabayashi, 2011; 2012; 2015). Serpentinites generally occur either as intact sheets of abyssal peridotite derived from the subducting plate

(Coleman, 2000; Wakabayashi, 2004; Prohoroff et al., 2012) or as detrital serpentinite mélanges that originated as debris flows which were deposited in the trench from the upper plate (Wakabayashi, 2012; 2015).

### *2.1. High-grade metamorphism in the Franciscan Complex*

About one-fourth of the exposed rocks in the Franciscan Complex have been subjected to high-pressure/low-temperature (HP-LT) lawsonite-albite, blueschist, or higher-grade metamorphism while the remaining rocks are of prehnite-pumpellyite or zeolite grade (Blake et al., 1984, 1988; Ernst and McLaughlin 2012). High-grade metamorphic rocks including coarse-grained recrystallized blueschist, amphibolite, garnet-amphibolite, and eclogite form a small volume (<<1%) of the Franciscan. These most often occur as exotic blocks within mélange horizons throughout the accretionary complex (Coleman and Lanphere, 1971), but also as rare coherent fault-bounded sheets, up to 1.5 x 2 km in size with maximum thicknesses of hundreds of meters, that occupy the highest structural levels in the Franciscan (Wakabayashi and Dumitru, 2007; Wakabayashi et al., 2010).

High-T garnet-amphibolites have experienced estimated maximum metamorphic temperatures of 550 – 630 °C (Tsujimori et al., 2006; Mulcahy et al., 2014), while lower-grade epidote-bearing blueschists formed at 300 – 350 °C (Ukar and Cloos, 2014). Reported metamorphic pressures for high-grade rocks have ranged from < 0.4 GPa for garnet-free amphibolites (Wakabayashi, 1990) up to 1.6 – 2.5 GPa for eclogites (Tsujimori et al., 2006; Page et al., 2007). However, more recent reanalysis of low-P amphibolites reported by Wakabayashi (1990) has returned pressures of >1 GPa (Wakabayashi, 2015), thus indicating that all high-grade rocks within the Franciscan Complex formed under HP conditions.

The metamorphic ages of the high-grade rocks are the oldest in the Franciscan. Recent analyses have returned Lu-Hf garnet and U-Pb Zircon ages as old as ~176 Ma for peak eclogite facies metamorphism (Mulcahy et al., 2018), and <sup>40</sup>Ar/<sup>39</sup>Ar hornblende ages of 168 – 157 Ma (Rutte et al., 2020). These ages overlap with previous dating results for both high-grade blocks and coherent sheets (e.g. Ross and Sharp, 1988; Wakabayashi and Dumitru, 2007). It is likely that this early phase of high-T metamorphism is representative of the elevated geothermal gradient present at the onset of subduction with respect to normal HP-LT subduction conditions (e.g. Platt, 1975). Notably, maximum metamorphic temperatures apparently decrease with age,

with 154 – 120 Ma epidote blueschists (Wakabayashi and Dumitru, 2007) formed at temperatures of 300 – 400 °C (Blake et al., 1988; Cooper et al., 2011), ~120 – 80 Ma lawsonite blueschist facies rocks (Wakabayashi and Dumitru, 2007) formed at 150 – 250 °C, and ~100 – 15 Ma prehnite-pumpellyite and zeolite facies rocks formed at <250 °C (Blake et al., 1988; Ernst and McLaughlin, 2012).

## 2.2. *Origins of Franciscan mélanges*

Mélanges comprising blocks enclosed in a mud, serpentinite, or mixed mud-serpentinite matrix are a volumetrically major portion of the Franciscan Complex. The origin of mélanges has been the subject of much confusion over the past few decades and has primarily centered on a commonly observed deformational fabric in mélange matrix (Cowan, 1985) which has resulted in a tectonic versus sedimentary debate (Wakabayashi, 2015). Moreover, the occurrence of high-grade blocks up to eclogite facies in low-grade matrix requires a process that is also responsible for the deep exhumation of high-grade material (Figure 2). Using numerical modeling, Cloos (1982) proposed the existence of a narrow corner flow region at the subduction interface which would cycle mud mélange matrix to depths of ~40 km before returning to the surface (Figure 3). High-grade blocks could be plucked from the upper-plate and entrained within the laminar flow, with their chaotic mixing a function of density settling in the flowing mélange matrix (Cloos, 1982; Cloos and Shreve, 1988b). In this scenario, the metamorphic discrepancy between high-grade blocks and low-grade matrix is explained by the ‘sinking’ of dense blocks in upwelling mélange resulting in their horizontal displacement into matrix that has only reached progressively shallower levels (Cloos and Shreve, 1988b). Gerya et al. (2002) expanded on the original subduction channel idea by incorporating serpentinite as the dominant matrix.

While the subduction channel model has been a popular interpretation of the Franciscan mélanges (e.g. Grigg et al. 2012), and has since been applied to subduction zones around the world, recent field and petrographic studies of several well-exposed mélange bodies have identified sedimentary structures in siliciclastic and serpentinite matrix mélanges, in addition to local zones lacking deformation (e.g. Platt, 2015; Wakabayashi, 2015, 2017, 2021a, 2021b). These observations suggest a sedimentary interpretation, with the exhumation of high-grade rocks occurring prior to mass wasting, chaotic deposition as a debris flow, and subsequent deformational overprinting (subduction-accretion). This interpretation has been strengthened by

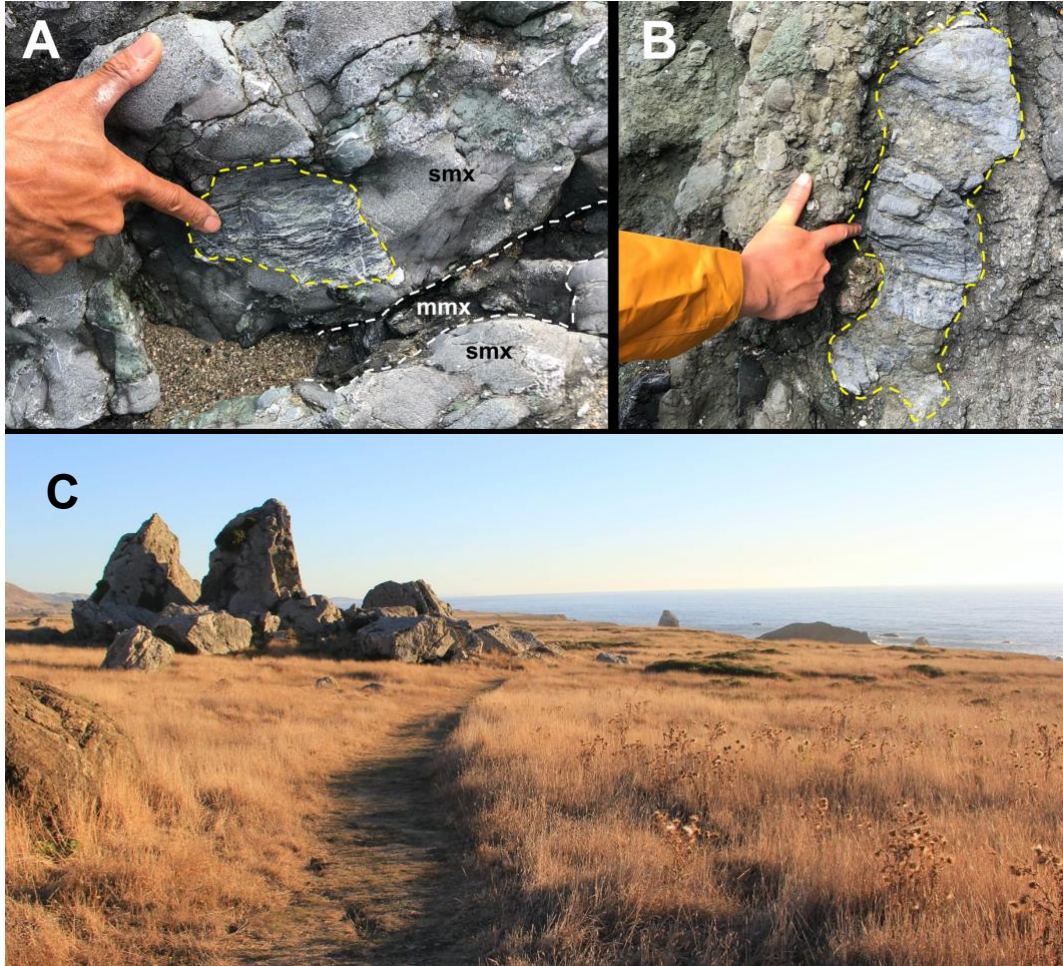


Figure 2. High-grade blocks in mélangé at North Shell Beach, northern California. A) Coarse blueschist clast within interfingered sand matrix (smx) and mud matrix (mmx) mélangé. B) Elongated coarse blueschist clast within mud matrix with a prominent foliation. C) In-situ garnet-amphibolite (~10 m tall, middle) and eclogite boulders on the terrace above the sea-cliff exposures shown in A and B.

progressive developments in seafloor imaging which have revealed mass wasting to be a common process in subduction zones due to the continuous tectonic oversteepening of terrain above the trench (e.g. Claussmann et al. 2021).

Diapiric serpentinite intrusions, analogous to the serpentinite mud volcanoes of the Marianas forearc (e.g. Fryer et al., 1999, 2000; Maekawa et al., 2008), have also been suggested as a source for serpentinite matrix mélanges (e.g. Tsujimori et al., 2007, Wakabayashi, 2015). However, identification of diapiric mélanges is challenging due to the difficulty in proving that the mélangé matrix has clearly moved upwards relative to surrounding host rock (e.g. Orange, 1990). Serpentinite-rich olistostrome horizons at the base of the GVG host high-grade blocks equivalent to those found in Franciscan mélanges. These deposits are claimed to have been

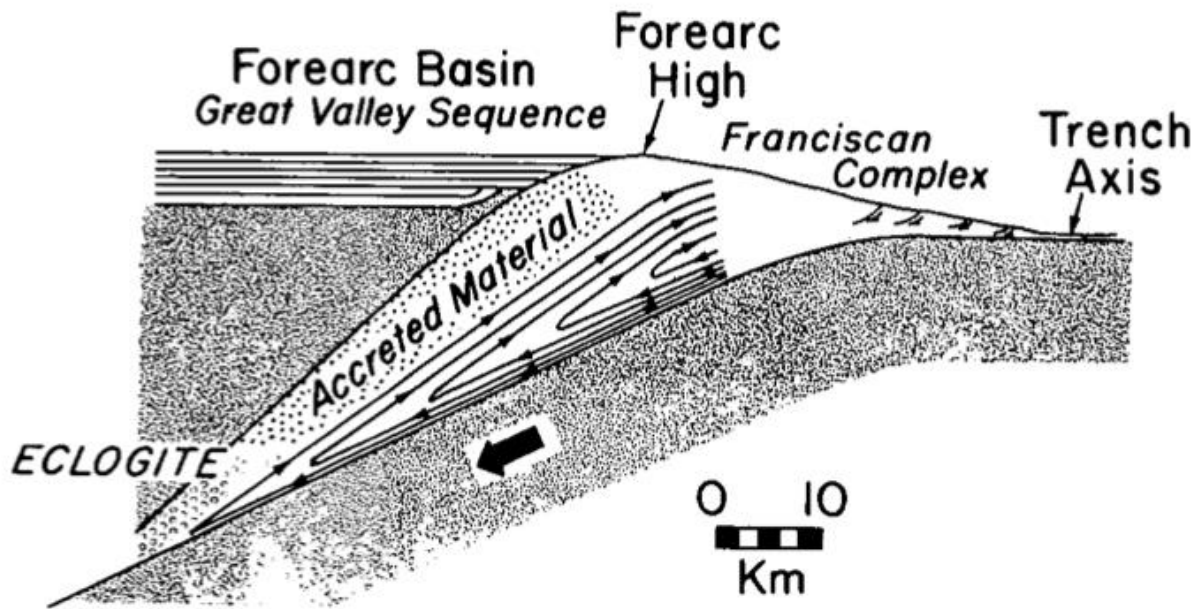


Figure 3. Schematic of a subduction channel corner flow. Note the cycle of matrix to depths of ~40 km after which it may incorporate rocks of varying metamorphic grade from previously accreted material on the upper plate. From Cloos, 1982.

sourced by serpentinite diapirs that accommodated exhumation of high-grade blocks early in the history of the Franciscan (Wakabayashi and Hitz, 2012). Actual preserved serpentinite diapirs have been described in the Franciscan (e.g. Dickinson, 1966; Cowan and Mansfield, 1970; Tsujimori et al., 2007) but none with a genetic relationship to concurrent subduction in the Franciscan have been definitively characterized.

### 3. Raman Spectroscopy of Carbonaceous Material as a Thermometry Method

The process of graphitization, the conversion of poorly ordered carbonaceous material (CM) to graphite, is well-characterized by Raman spectroscopy (e.g. Tuinstra and Koenig, 1970; Wopenka and Pasteris, 1993; Beyssac et al., 2002). The first-order Raman spectrum of CM in the 1100 – 1700  $\text{cm}^{-1}$  wavenumber window has two main intensity bands. The prominent graphite band (G-band) at ~1575  $\text{cm}^{-1}$  is an  $E_{2g}$  mode corresponding to in-plane vibrations within the graphite crystal lattice (Tuinstra and Koenig, 1970). In more disordered CM, a decrease in crystallite size  $L_a$  results in the appearance of two disorder-induced bands at ~1350  $\text{cm}^{-1}$  (D-band) and ~1620  $\text{cm}^{-1}$  (D'-band) (Wopenka and Pasteris, 1993). Tuinstra and Koenig (1970) assigned the D-band to an  $A_{1g}$  mode resulting from finite crystal size, with its intensity inversely

proportional to the crystallite size  $L_a$  in the direction of the graphite plane. In very disordered CM, the D'-band cannot be resolved from the G-band, and they combine to form a single broad peak at  $\sim 1600 \text{ cm}^{-1}$ .

Beysac et al. (2002) determined that graphitization of CM in metasedimentary rocks was strongly dependent on maximum metamorphic temperature but not on metamorphic pressure. This observation formed the basis of a thermometer using the R2 parameter, a ratio of peak areas for the disordered and ordered bands, which works well over a metamorphic temperature range of 330 – 650 °C. Raman spectroscopy of CM (RSCM) is an especially desirable method as it is nondestructive with minimal sample preparation required. Other researchers have attempted to extend the RSCM thermometer to diagenetic temperatures (e.g. Rahl et al., 2005; Lahfid et al., 2010). Like the original method pioneered by Beysac et al. (2002), these empirical techniques usually involve the comparison of parameter ratios originating from various curve fitting strategies. Developing upon these earlier thermometer calibrations, Lünsdorf et al. (2017) recognized the prevalence of operator bias in curve fitting methods and implemented a more standardized approach using a reference sample series and an automated curve-fitting routine (Lünsdorf and Lünsdorf, 2016) aimed at limiting biases introduced during spectral processing.

Retrograde metamorphic events have been shown to have no effect on graphitization of CM, and thus the process is apparently irreversible (Beysac et al., 2002). However, it is worth considering that graphitization is a kinetically controlled process and metamorphic temperatures change on the order of millions of years. Similar kinetically driven processes indicate that reaction rate increases non-linearly with increasing temperature (Dodson, 1976; Baxter, 2003), and thus graphitization is probably highly influenced by the duration of time at maximum temperature (Rahl et al., 2005). Since the RSCM method is calibrated by samples with temperatures constrained from metamorphic petrology, the resultant temperatures are best understood as 'maximum metamorphic temperatures' as they represent estimates tied to results that would be obtained by other metamorphic thermometry methods.

#### **4. Data Acquisition and Treatment**

Raman spectroscopy of carbonaceous material (RSCM) was conducted on standard petrographic thin sections for both the calibration dataset and the Franciscan samples. Spectra were acquired with a LABRAM HR800 micro-Raman spectrometer using a Nd:YAG 532 nm

laser source and a Peltier-cooled CCD detector with the LabSpec5 software. A 300 nm confocal hole was used to focus the laser beam on the sample using a 100x objective. A slit size of 200 nm and grating of 1200 were also used for the Raman measurements.

For each sample, 10 independent spot measurements were collected for 60 s intervals. A spectral window of 800 – 2000  $\text{cm}^{-1}$  was used to allow for adequate baseline estimation. The MATLAB program *meanRaman* was developed to obtain a representative spectrum for each sample. Each of the 10 spot spectra for a given sample were baseline-corrected using the non-quadratic cost function algorithm of Mazet et al. (2005), normalized relative to the mean intensity, and reduced to a spectral window of 1125 – 1700  $\text{cm}^{-1}$  to eliminate contribution of peaks from other mineral phases (e.g. calcite). The mean profile of the baseline-corrected and normalized spectra serves as the representative spectrum for a sample. Also reported for each sample is the reduced chi-square value,  $\chi_r^2$ . This compares the variance of individual spectra around the representative mean profile relative to the variance expected for a Poisson process ( $\chi_r^2 = 1$ ) and thus provides a measure of sample heterogeneity.

It is worth noting uncertainty sources that may result in inhomogeneous spectra for a given sample. The plane of polarization of the laser beam has been shown to induce geometry-sensitive effects relating to grain orientation, with D- and G-band intensity ratios affected by the resulting scattering geometry (e.g. Wopenka and Pasteris, 1993). The effects of this anisotropy may be mitigated by use of a quarter-wave plate, but common practice has been to reduce its influence by measuring CM grains in oriented thin sections or rock chips that are cut normal to any macroscopic foliation and parallel to any stretching lineation (Beyssac et al., 2002). In addition, polishing and other mechanical effects imparted during sample preparation have also been claimed to induce disorder in more graphitic samples (e.g. Nakamizo et al., 1978). However, the effects of this are likely minimal, and Wopenka and Pasteris (1993) observed no differences between the Raman spectra of ball-milled graphite and granulite-grade graphite. Finally, geological effects come into play with the potential for inherent sample heterogeneity due to naturally inhomogeneous crystallite sizes. Also, the incorporation of detrital CM grains with different thermal histories is worth consideration as these introduce outlier spectra of comparatively higher-T with respect to the actual maximum metamorphic temperature of the sample. Thus, in obtaining a representative spectrum for a heterogenous sample, it may be beneficial to focus on the spectra that comprise the lowest temperature population of the CM

grains. However, this was avoided in the current study as we wanted to observe general heterogeneity across our samples, and the final calibration dataset remained stable even without omitting the occasional outlier spectra.

#### 4.1. Calibration samples

A calibration dataset of samples with independently known maximum metamorphic temperatures (Table 1) was obtained from two sources: 1) the central and western Alps reference series of Lünsdorf et al. (2017) and 2) vitrinite samples from the Suviana 1 well in the Apennines (Anelli et al., 1994). The Lünsdorf et al. (2017) reference sample series was developed with the following criteria in order of decreasing importance: a) independent and well-defined maximum metamorphic temperature, b) unweathered, c) homogenous CM spectra, and d) sample accessibility (Lünsdorf et al., 2017). Keno Lünsdorf of the University of Göttingen provided us with 24 of the 26 samples present in the original reference series which span a temperature range of 162 – 610 °C.

The Suviana 1 well was drilled as part of a petroleum exploration project in the Northern Apennines of Italy (Anelli et al., 1994). Drilling reached a corrected depth of 7131 m. Vitrinite samples were provided by Sveva Corrado of University Roma Tre from 13 locations in the well, between 300 and 5970 m (uncorrected depth). The well deviates from vertical below 4 km depth (Verdoya et al., 2019). Table A shows both the original reported depths for the samples and their corrected depths, along with estimated maximum temperatures. The maximum temperatures were estimated by using vitrinite measurements ( $n = 49$ ) reported in Anelli et al. (1994, Fig. 5). Figure 4A shows that the vitrinite reflectance,  $R_{0, \text{median}}$ , increases monotonically with depth and Figure 4B shows the conversion of these  $R_{0, \text{median}}$  values to  $T_{\text{max}}$  values using the calibration of Barker and Goldstein (1990). These  $T_{\text{max}}$  values were smoothed using a spline function, and then used to estimate the  $T_{\text{max}}$  values for the provided vitrinite samples. As a check, Figure 4B also shows modern temperature estimates 195 and 214 °C for two corrected depths in the well, 6029 and 6491 m respectively, as reported by Verdoya et al. (2019, Table 1a). The vitrinite samples (Anelli et al., 1994) indicate that samples with  $T_{\text{max}}$  equal to these modern temperatures presently lie 4.7 km above these modern temperature estimates. This difference is due to erosion, which has allowed the geologic units to move upward relative to the Earth's surface. Zattin et al. (2002,

Table 1. PLS Regression Calibration Samples for RSCM Thermometry

Sample	$T_{max}$ (°C)	Method <sup>b</sup>	Reference <sup>c</sup>	$\Delta T_{PLS}$ <sup>d</sup> (°C)	$\chi^2_r$
suv300	156 ± 20	1	A	-26.8	4.9
KL14-5A	162 ± 30	3	B	-26.4	6.7
suv805	165 ± 20	1	A	8.6	1.3
suv1315	177 ± 20	1	A	0.5	1.9
KL14-7	178 ± 30	3	B	-3.6	7.8
suv1800	215 ± 20	1	A	13.2	1.2
KL14-21	228 ± 30	3	B	-12.1	5.9
suv2300	231 ± 20	1	A	0.0	0.9
KL14-16A	236 ± 30	3	B	-7.3	23.3
KL16-31	236 ± 30	3	C	-15.4	17.3
KL16-35	240 ± 30	3	C	7.9	43.6
suv2800	240 ± 20	1	A	3.1	0.9
suv3300	248 ± 20	1	A	2.3	1.3
KL14-17	256 ± 30	3	B	-22.6	43.8
KL16-43B	262 ± 30	3	C	-22.5	4.3
KL14-13A	267 ± 30	3	B	-18.2	12.1
suv3805	268 ± 20	1	A	27.0	1.2
suv4300	278 ± 20	1	A	10.7	5.5
KL14-1A	295 ± 20	2	B	-2.4	2.2
suv4810	297 ± 20	1	A	21.6	1.1
KL14-19	299 ± 23	2	B	11.7	7.5
suv5670	303 ± 20	1	A	0.1	0.7
suv5970	309 ± 20	1	A	16.8	3.7
suv5270	311 ± 20	1	A	16.9	1.3
KL16-8B	325 ± 25	5	F	18.6	30.7
KL16-19B	350 ± 25	5	F	-4.3	10.3
KL14-58B	370 ± 50	4	D	-14.1	11.0
KL16-10B	375 ± 35	5	F	9.1	12.7
KL16-14	415 ± 35	5	F	-3.4	18.8
KL14-59	420 ± 50	4	D	-26.4	9.2
KL16-29	420 ± 30	4	D	-5.4	15.5
KL16-27	440 ± 30	4	D	7.7	27.9
KL14-56B	450 ± 30	4	D	44.4	11.3
KL16-23	480 ± 40	5	D/E	-33.7	14.9
KL16-16B	490 ± 40	5	F	27.9	15.5
KL14-52	520 ± 25	4, 5	D/E	-5.8	12.9
KL14-49C	610 ± 50	4, 5	D/E	2.3	12.7

<sup>a</sup> For vitrinite samples obtained from the Suviana 1 well, an uncertainty on the order of ± 20 °C is inferred from the calibration of Barker and Goldstein (1990, Fig. 2).

<sup>b</sup> 1: vitrinite reflectance; 2: fluid inclusion homogenisation temperature; 3: calcite-dolomite thermometry; 4: pressure-temperature estimation by multi-equilibrium calculation.

<sup>c</sup> A: Anelli et al. (1994), Barker and Goldstein (1990), see Section 4.1; B: Rahn (1996); C: Frey (1987); D: Lünsdorf et al. (2017); E: Todd and Engi (1997); F: Agard et al. (2001).

<sup>d</sup> Difference between observed and predicted temperature using the PLS calibration fit for the dataset. See Figure 6D.

<sup>e</sup> Reduced chi-square

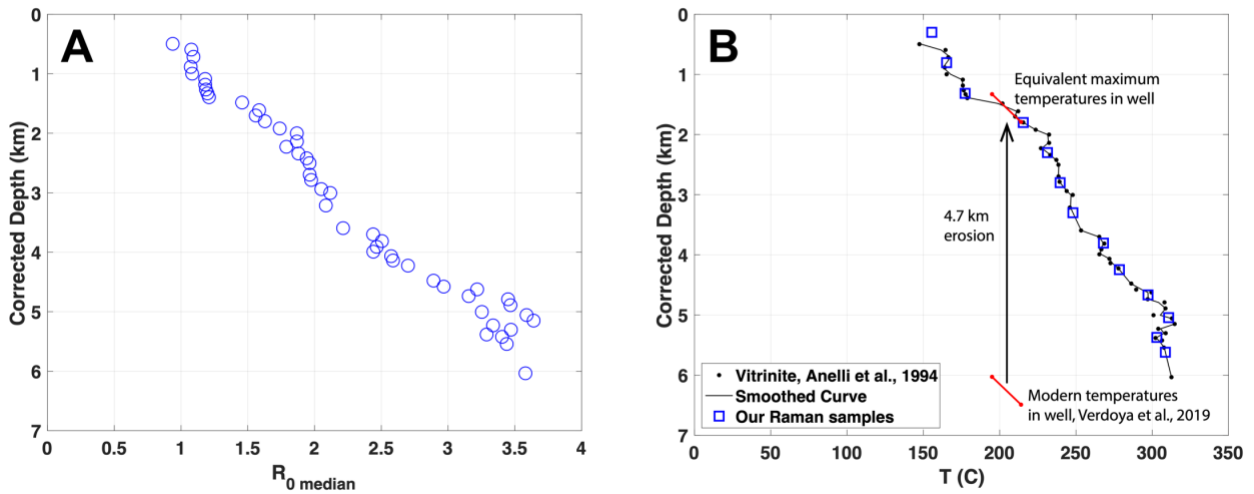


Figure 4. Vitrinite reflectance data for the Suviana 1 well in the Apennines, Italy. A) Corrected well depth versus vitrinite reflectance  $R_{0,median}$  from Anelli et al. (1994). B) Corrected well depth versus maximum metamorphic temperatures  $T$  for Anelli et al. (1994) vitrinite samples, smoothed with a spline function, and our calibration samples using the vitrinite thermometer of Barker and Goldstein (1990). Also plotted are modern temperature estimates for two corrected well depths, consistent with regional estimates for erosion (Zattin et al., 2002).

Fig. 16) gives a similar estimate for total erosion in this area. The Suviana 1 well samples span a temperature range of 156 – 311 °C.

The combined spectral calibration dataset ( $n = 37$ ) is shown graphically plotted against corresponding temperatures in Figure 5. Remarkably, a continuous trend is clearly discernable, and mirrors reports from previous studies (Tuinstra and Koenig, 1970; Lünsdorf et al., 2017). At temperatures  $< 200$  °C the D-band is wide with additional shoulders at lower and higher wavenumbers. The G-band is also wide and the maximum D-band intensity  $D_{max}$  is about half of the maximum G-band intensity,  $G_{max}$ . A low temperature zone between  $\sim 200 - 300$  °C is characterized by the progressive decrease in D-band width and disappearance of the low-T shoulders, as well as a relative increase in  $D_{max}$  such that  $D_{max}/G_{max} \approx 1$  at  $\sim 300$  °C. In a transition zone between  $\sim 300 - 400$  °C, the D-band, initially centered at  $\sim 1340$   $\text{cm}^{-1}$ , eclipses the G-band and reaches a maximum relative intensity of  $D_{max}/G_{max} \approx 1.8$  at  $\sim 375$  °C while shifting to  $\sim 1360$   $\text{cm}^{-1}$ . During this same interval the G-band, initially centered at  $\sim 1600$   $\text{cm}^{-1}$ , develops a shoulder at  $\sim 1620$   $\text{cm}^{-1}$  (the D'-band) and shifts to  $\sim 1585$   $\text{cm}^{-1}$ . The intensity ratio undergoes a second inversion at  $\sim 400$  °C with the relative G-band intensity increasing to  $D_{max}/G_{max} \approx 0.9$  at  $\sim 415$  °C. This transition zone interval apparently corresponds to the

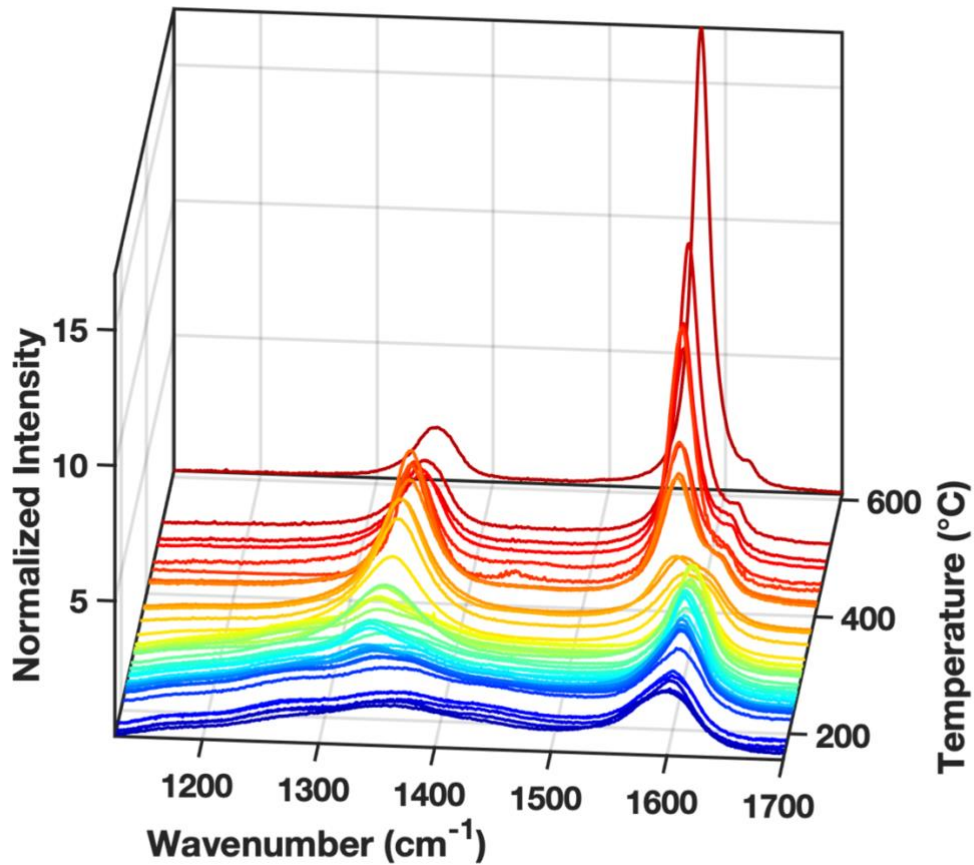


Figure 5. Calibration dataset used for PLS regression RSCM thermometry. Intensity is normalized to the mean intensity of each sample. Corresponding samples are tabulated in Table 1.

conversion of most of the CM to microcrystalline graphite (Tuinstra and Koenig, 1970; Lünsdorf et al., 2017). A high temperature zone between  $\sim 400 - 610$  °C is characterized by a continuous increase in  $G_{max}$  and corresponding decrease in  $D_{max}$ , which is related to the general trend based on increasing graphite crystallite size  $L_a$  that was originally exploited by Beyssac et al. (2002) in the first RSCM thermometer.

#### 4.2. RSCM thermometry with Partial Least Squares (PLS) regression

Partial least squares (PLS) regression is a linear modeling tool that has seen widespread application in chemometrics (Wold et al., 2001). This method is particularly useful as it can analyze data with many interrelated and noisy ‘predictor’ variables and map them to associated

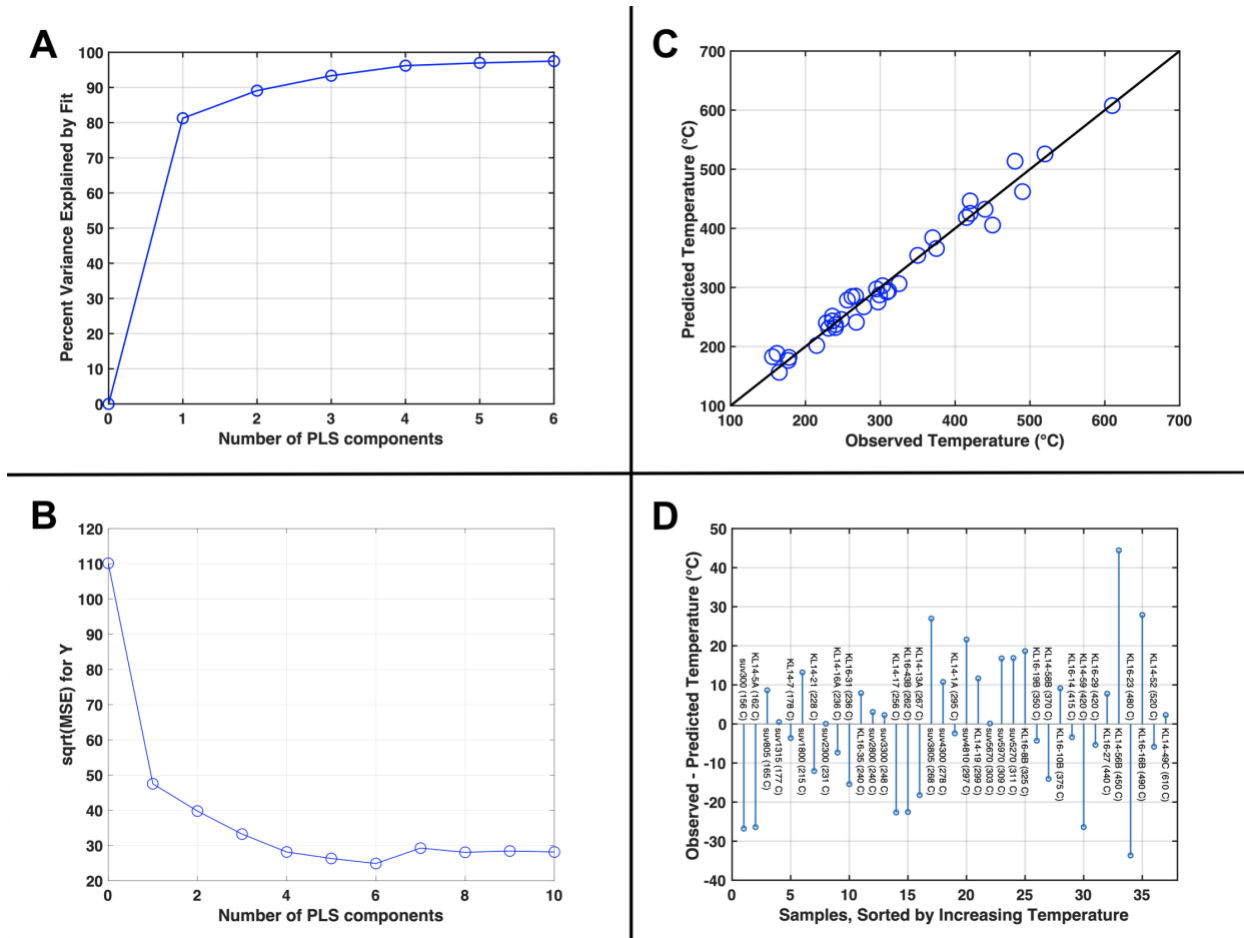


Figure 6. PLS regression fitting of the calibration data set. The model has a standard error of  $\pm 17$  °C and a  $R^2$  value of 0.97. A) Percent variance explained by the PLS fit versus the number of PLS components used. B) Estimated mean squared prediction error (MSE, plotted as its square root) for temperature (denoted with Y) using 10-fold CV with the program *plsregress* in MATLAB versus the number of PLS components used. Six PLS components is shown to minimize this quantity. C) Predicted versus observed temperatures using the PLS calibration fit. D) Difference between observed and predicted temperatures for each sample in the calibration dataset.

‘response’ variables. PLS regression achieves this by reducing the dimension of the regression problem from many predictor variables to a small set of orthogonal linear combinations of predictor variables, or ‘components’. The technique lends itself well to spectral analysis where it has been used to fit a variety of spectral data to different response variables (e.g. Killner et al., 2011). Thus, PLS regression offers a new approach to RSCM thermometry that completely avoids operator bias inherent in traditional parameter-based, curve fitting methods.

Here we present a PLS regression model for RSCM thermometry based upon the calibration dataset shown in Table 1. This model was generated in MATLAB using the *plsregress* program and was applied to our calibration dataset to generate a 6-component PLS

model, the results of which are shown in Figure 6. To determine the number of components that maximized predictive power without overfitting the data, 10-fold cross-validation (CV) was used to find the number of components that minimized the mean squared prediction error (MSE) (Figure 6B). The final PLS fit for our RSCM calibration dataset has an R-squared value of 0.97 and a standard error of  $\pm 17$  °C.

## 5. Franciscan Samples

For the current reconnaissance thermometry study, 12 samples of siliciclastic mélangé matrix, 4 samples of sandstone, and 4 samples with uncertain block-matrix character were gathered from six localities across the Franciscan Complex (Table 2). At North Shell Beach, matrix samples SB210729-1, 3, and 6 were obtained from an outcrop displaying interfingering of mud and sand matrix mélangé hosting high-grade blocks (Figure 2A,B), adjacent to a similar outcrop described by Wakabayashi (2015, Figs. 16d,e). Samples SB210726-1, and 2 were obtained from the contact of a large ~60 m garnet-amphibolite block depicted by Wakabayashi (2021b, Fig. 12A-D), with the former coming from a clastic serpentinite-rich selvage in contact with the block (Wakabayashi, 2021b, Fig. 12B,C). A similar sample (GR210726-2) was gathered to the north near Goat Rock from a serpentinite-mud mélangé body carrying abundant cm to dm scale blueschist clasts. Petrographic observations of these samples confirmed the serpentinite-rich character of the matrix in contrast with typical mud matrix samples (Figure 7A-F). At Mount Diablo, matrix was gathered from a ~0.5 deformed mélangé horizon hosting a garnetite block described by Wakabayashi (2021a, Fig. 5A-D, 2021b, Fig. 10E-F). Samples SRW210728-1, and 2 were obtained from a mélangé outcrop in the Sunol Regional Wilderness depicted by Wakabayashi (2017, Fig. 10l). Samples DR-53, and 161 were provided by Darrel Cowan and gathered from a mélangé body in Mustang Canyon north of Pacheco Pass in the Diablo Range (Cowan, 1972). Sample 75S-5 was also provided by Darrel Cowan and gathered from a mélangé body near San Simeon pier (Cowan, 1978).

Four samples from coherent sandstone units at North Shell Beach, Goat Rock, Mount Diablo, and Sunol were obtained for comparison. Additionally, samples MD210727-3 from Mount Diablo and SRW210728-4, 5, and 6 from Sunol were gathered from siliciclastic outcrops adjacent to large high-grade blocks, but without clear exposure of block-matrix contacts. Hence, it was uncertain whether these samples constitute mélangé matrix or sandstone blocks within

Table 2. Franciscan Siliciclastic Raman Thermometry Samples and Results

Sample <sup>a</sup>	Locality	Outcrop Description	$T_{max}$ (°C)	$\chi_r^2$
<i>Mud matrix mélange</i>				
SB210726-2	North Shell Beach	Mud-sand matrix in contact with ~60 m garnet-amphibolite block. <sup>b</sup>	211	1.7
SB210729-1	“	Mud matrix with coarse blueschist and ultramafic clasts. <sup>c</sup>	191	2.4
SB210729-3	“	As SB210729-1. <sup>c</sup>	190	3.3
SB210729-6	“	Sand matrix mélange. Interfingered with mud matrix. <sup>c</sup>	190	1.8
MD210727-1	Mount Diablo	~0.5 m thick mud horizon enclosing ~0.5 m long garnetite block. <sup>d</sup>	238	5.8
SRW210728-1	Sunol Regional Wilderness	Mud matrix. Gradational contact with sandstone. <sup>e</sup>	207	3.1
SRW210728-2	“	As SRW210728-1. <sup>e</sup>	215	2.5
DR-53	Diablo Range	n/a	208	3.5
DR-161	“	n/a	219	2.4
75S-5	San Simeon	n/a	204	1.6
<i>Serpentinite-mud matrix mélange</i>				
SB210726-1	North Shell Beach	Serpentinite-mud matrix in contact with ~60 m garnet-amphibolite block. <sup>b</sup>	382	4.9
GR210726-2	Goat Rock (Blind Beach)	Serpentinite-mud matrix with coarse blueschist clasts.	392	2.6
<i>Sandstones</i>				
SB210729-2	North Shell Beach	Muddy turbidite from coherent sandstone body near Peaked Hill.	289	33.8
GR210726-1	Goat Rock (Blind Beach)	Turbidite sandstone interbedded with cm scale mudstone layers.	247	56.4
MD210727-2	Mount Diablo	Sandstone horizon below MD210727-1. <sup>c</sup>	210	60.1
SRW210728-3	Sunol Regional Wilderness	From large coherent sandstone sheet.	278	76.2
<i>Unknown block-matrix relationships</i>				
MD210727-3	Mount Diablo	Siliciclastic (matrix?) adjacent to ~50 m garnet-amphibolite/eclogite block.	265	4.4
SRW210728-4	Sunol Regional Wilderness	“ “ “ ~ 5 m amphibolite block.	276	21.3
SRW210728-5	“	“ “ ~7 m to W of ~5 m garnet-amphibolite/eclogite block.	204	5.2
SRW210728-6	“	“ “ ~6 m to N of ~5 m garnet-amphibolite/eclogite block.	279	26.1

<sup>a</sup> Specific sample locations are provided in Supplementary Information Table S1. Samples DR-53 and DR-161 were collected by Darrel Cowan from a mélange body in Mustang Canyon north of Pacheco Pass (Cowan, 1972). Sample 75S-5 was also collected by Darrel Cowan from a mélange body near San Simeon pier (Cowan, 1978).

<sup>b</sup> Block contact depicted in Figure 20I, Wakabayashi 2015 and Figure 12A-D, Wakabayashi 2021b. <sup>c</sup> Outcrop adjacent to that depicted in Figures 16d,e, Wakabayashi 2015. <sup>d</sup> Same outcrop depicted in Figures 5A-D, Wakabayashi 2021a and Figure 10E, F, Wakabayashi 2021b. <sup>e</sup> Outcrop depicted in Figure 10I, Wakabayashi 2017.

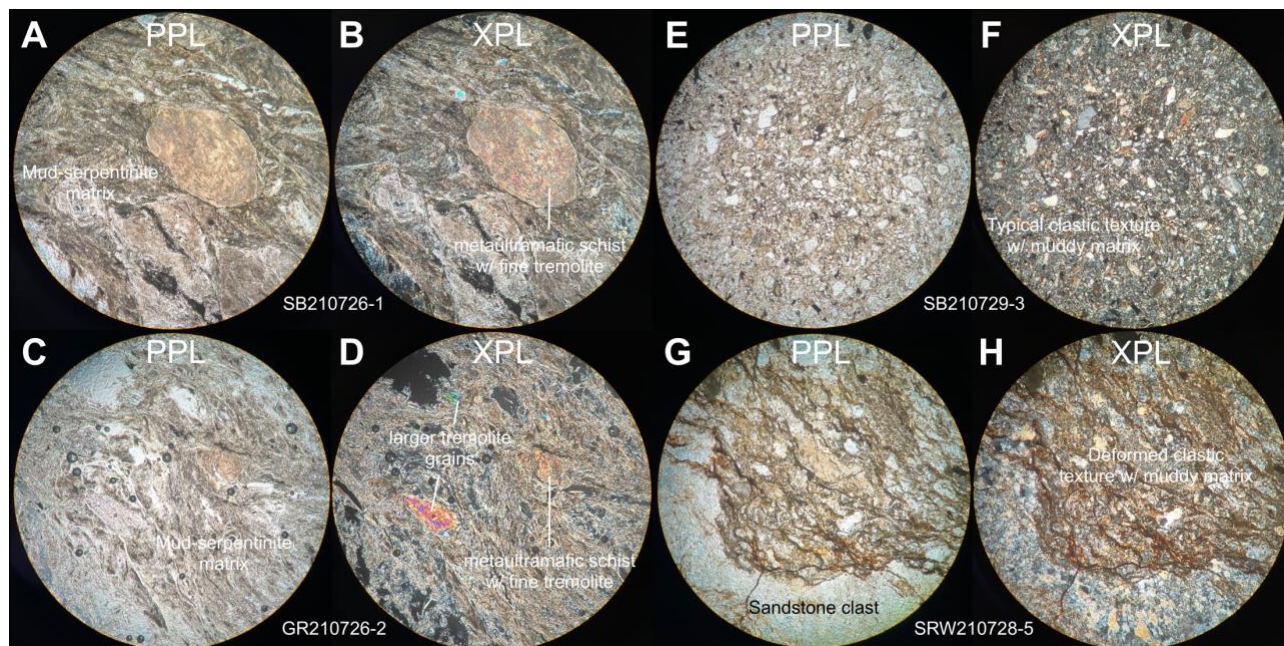


Figure 7. Photomicrographs of select mélangé matrix samples from the Franciscan. PPL indicates plane polarized light while XPL denotes cross polarized light. FOV is 3 mm. A, B) matrix (SB210726-1) from a serpentinite-rich selvage adjacent to a ~60 m garnet-amphibolite block at North Shell Beach described by Wakabayashi (2021b, Figure 12A-D). Clasts of metaultramafic schist composed of fine tremolite, as well as larger tremolite grains, are seen set in a deformed serpentinite-mud matrix. C, D) serpentinite-mud matrix (GR210726-2) from a mélangé body near Goat Rock. Characteristics are the same as those seen in A and B. E, F) Typical mud matrix from North Shell Beach characteristic of siliciclastic Franciscan mélanges. Here, the matrix is largely undeformed with a distinct clastic texture. G, H) Photomicrograph of a siliciclastic sample (SRW210728-5) obtained adjacent to a large garnet-eclogite block in the Sunol Regional Wilderness in the absence of clear block-matrix outcrop relationships. However, thin section reveals a deformed clastic texture with a muddy matrix, consistent with other siliciclastic mélangé outcrops.

mélangé, and these are categorized as such in Table 2. However, in thin section, sample SRW210728-5 had a clastic texture consistent with other matrix samples (Figure 7G,H). (Specific latitudes and longitudes for sample locations are provided in Supplementary Information Table S1.)

When collecting Raman spectra for mélangé matrix samples, special care was taken to ensure that CM grains within clearly identifiable mud matrix interstitial to clastic material were targeted by the micro-Raman spectrometer. This was done to limit the contribution of any anomalous higher-T detrital CM grains that may have been incorporated into the matrix and ensure an accurate representation of the maximum metamorphic temperature of the sample.

## 6. Synthesis of Results

The PLS Raman thermometry results for the Franciscan samples are tabulated in Table 2. Notably, maximum metamorphic temperatures for mélangé matrix samples from all 6 locations across the Franciscan fall within a narrow range of ~190 – 220 °C, with the exception of sample MD210727-1 from the ~0.5 m deformed mélangé horizon at Mount Diablo previously described by Wakabayashi (2021a, 2021b) which gave a temperature of 238 °C. Also of note is the homogeneity of individual spectra for each sample with  $\chi_r^2$  values generally in the 1.6 – 3.5 range (Figure 8A-D). The spectra of MD210727-1 were observed to contain a few outliers, as evidenced by a relatively high  $\chi_r^2$  value of 5.8. After removal of four anomalous spectra, a temperature of 234 °C was still returned for the new mean spectrum which proved that this was not an artifact of outliers. The slightly higher temperature of the prevalently deformed matrix of MD210727-1 (see Wakabayashi, 2021b, Figure 13A,B) with respect to the other samples may be reconciled with the observation of Barzoi (2015) that strain energy, even at thin section scale, promotes graphitization and can overestimate temperatures by up to ~150 °C using the RSCM thermometer of Beyssac et al. (2002). Hence, temperature estimates reported in this study may even overestimate maximum metamorphic temperatures depending on sample deformation.

A surprising result was returned from the two distinct serpentinite-rich mélangé matrix samples from the neighboring North Shell Beach (SB210726-1) and Goat Rock (GR210726-2) localities which gave high temperatures of 382 and 392 °C respectively (Figure 8E,F). The former sample is from a clastic serpentinite selvage adjacent to a large garnet-amphibolite block described by Wakabayashi (2021b). The spectral data for these samples were also relatively homogeneous with  $\chi_r^2 < 5.0$ . These samples share a petrography (Figure 7A-D) and thermal history distinct from the mud matrix mélangé samples of the Franciscan. For context, a serpentinite-free sample SB210726-2 was obtained about 1 meter away from SB210726-1 in contact with the same garnet-amphibolite block and returned a temperature of 211 °C.

The Franciscan sandstones differed drastically from the mélangé matrix samples in the heterogeneity of the obtained spectra with  $\chi_r^2$  values between 33.8 – 76.2 (Figure 8G,H). With this degree of spectral heterogeneity our mean profile based PLS-RSCM thermometry approach begins to break down in its predictive power, but the estimated ‘maximum metamorphic temperatures’ are still reported in Table 2. The sandstone temperatures are generally higher, which is undoubtedly the result of the incorporation of detrital high-T CM grains as can clearly

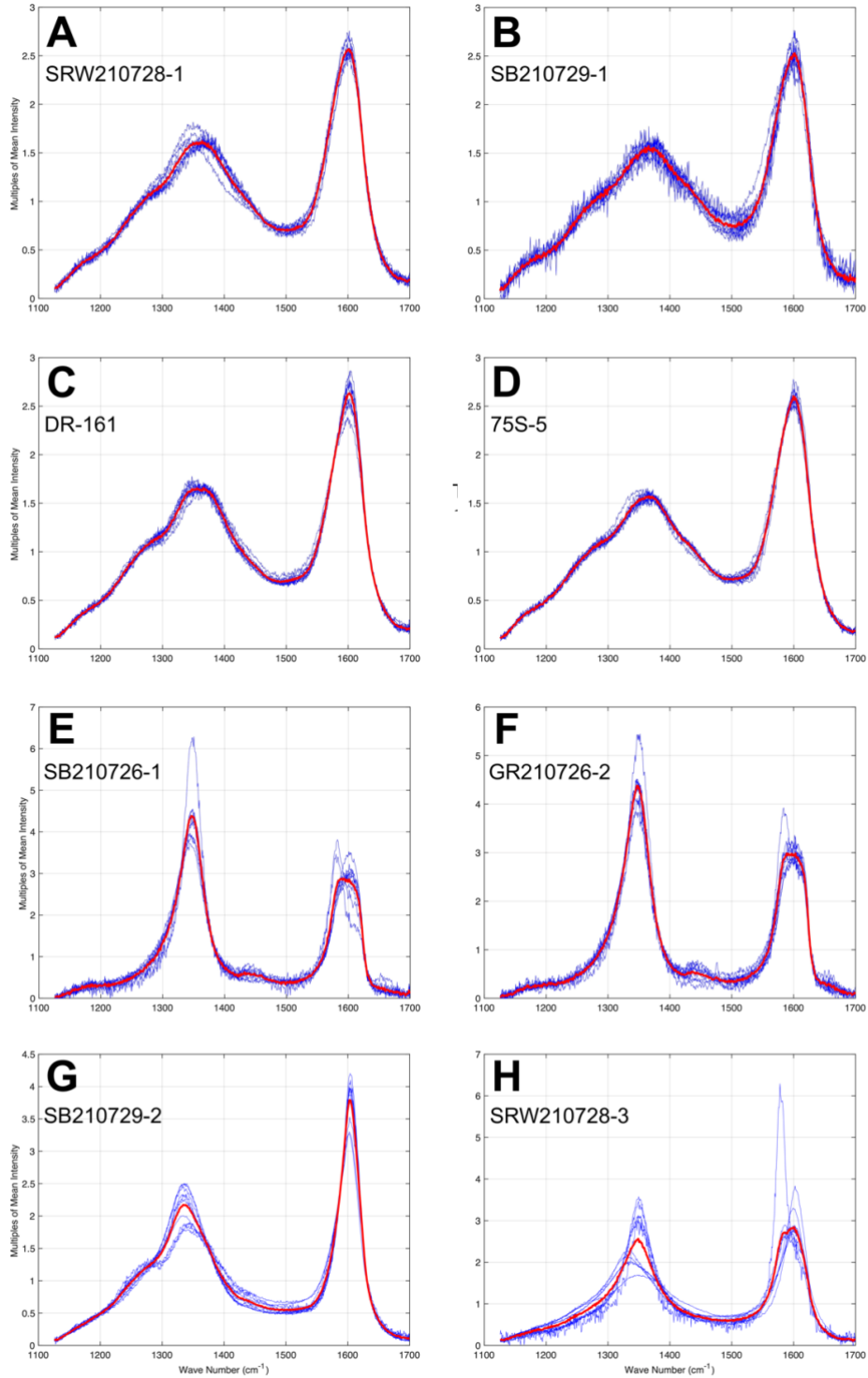


Figure 8. Representative Raman spectra for mud mélangé matrix (A-D), serpentinite-mud mélangé matrix (E, F), and sandstone (G, H) from locations across the Franciscan Complex. Individual spectra (blue) and the mean profile spectrum (red) are shown along with sample numbers. Sample  $T_{max}$  and  $\chi_r^2$  are the following. Mud matrix: A)  $T_{max} = 208$  °C,  $\chi_r^2 = 3.1$ ; B)  $T_{max} = 191$  °C,  $\chi_r^2 = 2.4$ ; C)  $T_{max} = 219$  °C,  $\chi_r^2 = 2.4$ ; D)  $T_{max} = 204$  °C,  $\chi_r^2 = 1.6$ . Serpentinite-mud matrix: E)  $T_{max} = 382$  °C,  $\chi_r^2 = 4.9$ ; F)  $T_{max} = 392$  °C,  $\chi_r^2 = 2.6$ . Sandstones: G)  $T_{max} = 289$  °C,  $\chi_r^2 = 33.8$ ; H)  $T_{max} = 278$  °C,  $\chi_r^2 = 76.2$ .

be seen in the spectra presented in Figure 8G,H. As mentioned in Section 4, it may be beneficial to isolate analysis on the spectra that comprise the lowest temperature population of the CM grains to accurately estimate maximum metamorphic temperatures, but adequate treatment of this issue requires more than 10 spot measurements per sample and was not conducted in our current reconnaissance study.

In the absence of exposed block and matrix relationships in outcrop, it is difficult to characterize a sample based on Raman analysis of a single thin section. Still, the estimated maximum temperatures are reported in Table 2 for the 4 samples obtained from siliciclastic outcrops adjacent to high-grade blocks. Sample SRW210728-5 from Sunol, obtained adjacent to a large garnet-amphibolite/eclogite block, appears to have mud matrix that shares a similar thermal history with matrix samples from other locations in the Franciscan with  $T_{max} = 204$  °C and  $\chi_r^2 = 5.2$ . This is consistent with petrographic observations shown in Figure 7G,H. The other 3 samples have higher temperatures and heterogeneous spectra consistent with the Franciscan sandstones, although the  $\chi_r^2$  value of 4.4 for MD210727-3 is quite homogenous compared to that of the other sandstones and perhaps represents a sample of a discrete sandstone block with a more uniform higher-T thermal history. Analysis of samples from mélangé outcrops with obscured or poorly characterized block-matrix relationships would benefit from more Raman measurements of CM grains across multiple thin sections for each rock sample, in addition to more detailed petrographic analysis.

## 7. Discussion

### 7.1. Low-temperature origins of mud matrix mélanges

This study confirms a large difference in metamorphic grade between the siliciclastic mélangé matrix in the Franciscan and the high-grade blocks the lie within the matrix. Matrix from a variety of locations across the Franciscan share remarkably similar maximum metamorphic temperatures around ~200 °C, and are commonly hosting blocks with metamorphic temperatures >550 °C. With these temperatures, the mélanges could have only reached depths of ~13 – 20 km assuming a geothermal gradient of 10 – 15 °C/km for the Franciscan Complex (e.g. Ernst, 1993).

The presence of high-grade blocks from depths of ~25 km for blueschists and ~50 km or greater for eclogites within a mud matrix that reached depths of 13 – 20 km is difficult to

reconcile with the subduction channel model. This was noted by Ukar (2012), who proposed that extensional thinning brought coherent underplated material from depths of <30 km up to 15 km, at which point they could have been incorporated into the subduction channel shear zone. This conclusion was reached based on observations at San Simeon, where the high-grade blocks comprise low-T epidote blueschists metamorphosed at ~15 – 20 km (Ukar, 2012; Ukar and Cloos, 2014). However, this does not account for the presence of garnet-amphibolite and eclogite blocks sourced from much greater depths at other mélangé localities where the metamorphic grade of the matrix is the same as that at San Simeon. In addition, Ring and Brandon (1994, 1999) used fault kinematic analysis and strain measurements to conclude that tectonic thinning had only a minor contribution to the exhumation of Franciscan units.

For tectonic mélanges originating in a subduction channel, matrix must have reached depths equivalent to those of the high-grade blocks, and one would expect to find a wide range of temperatures corresponding to matrix that upwelled from various depths. The range of maximum metamorphic temperatures for our mud matrix samples from different locations across the Franciscan is 190 – 238 °C, which is quite constrained in comparison with that reported for high-grade blocks (~300 – 630 °C). The absence of examples of high-grade mélangé matrix was noted by Cloos and Shreve (1988b). They suggested that matrix subducted to the greatest depths would be underplated at the deepest levels of the accretionary wedge. High-grade blocks, including eclogites, would be mixed by variable Stokes settling and move across streamlines towards the more rapidly upwelling portion of the subduction channel corner flow until they are surrounded and exhumed by matrix that reached much shallower depths (Cloos and Shreve, 1998b, Fig. 6). This poses some issues, as it does not explain the mixing of blocks with sizes on the order of ~1 m or less (or with comparatively low densities). Using the model of Cloos (1982), a 1 m diameter eclogite block would sink at a velocity of 1 m/Ma assuming a density contrast of 0.6 gm/cm<sup>3</sup> and matrix viscosity of 10<sup>16</sup> poise, which is negligible compared to a subduction velocity of 5 cm/yr (see Fig. 5 in Cloos, 1982). Subduction channel density settling would not appear to result in the observed chaotic mixing of blocks of varied sizes, densities, and metamorphic grade within mélangé bodies that have relatively uniform matrix temperatures of ~200 °C.

Sedimentary relationships at different mélangé localities have been well-documented (e.g. Platt, 2015; Wakabayashi, 2015). At North Shell Beach, interfingering of mud and sand matrix mélangé may be observed (Figure 2) and locally the matrix is undeformed. From this

locality, muddy regions within sand matrix mélange ( $T_{max} = 190$ , SB210729-6) returned equivalent temperatures to adjacent mud matrix mélange ( $T_{max} = 190$ , SB210729-1), suggesting that these units are syndepositional. The relatively uniform and low maximum metamorphic temperatures of matrix sampled in our study are consistent with a sedimentary interpretation of these mélanges as olistostromes. In this case, chaotic mixing of blocks is facilitated by large submarine debris flows sourcing a variety of rocks, including high-grade blocks, from higher-up the accretionary wedge. The uniform thermal history of CM grains results from the accumulation of CM by suspended mud as it settled through the water column. The apparent deformation (and local tectonic block-in-matrix texture) observed in mud matrix at these mélange localities would thus be a product of tectonic overprinting, and the observed maximum metamorphic temperatures of  $\sim 200$  °C in this study are a gauge of subsequent subduction and underplating of the trench fill deposits. The localization of post-depositional deformation during subduction-accretion in comparatively weak mélange matrix is unsurprising, and mélange horizons across the Franciscan appear to have accommodated this deformation in discrete zones up to  $\sim 300$  m thick (Wakabayashi, 2021b).

An argument against the sedimentary origin of mélanges in the Franciscan is the apparent lack of a high-grade source terrain at the time of mélange formation (Ukar, 2012). However, recycling of sedimentary material involving multiple episodes of subduction has been well-characterized in the Franciscan (e.g. Cowan and Page, 1975; Erickson et al., 2004; Erickson, 2011) and may explain observed temporal incongruities. High-grade blocks in the olistostromes of the basal GVG indicate the existence of a sedimentary source of high-grade material from the forearc high early in the history of the Franciscan (Hitz and Wakabayashi, 2012). Wakabayashi (2015) contends that these high-grade blocks, and the majority of those in the Franciscan, were exhumed as blocks-in-serpentine within serpentine diapirs. In addition, the structurally high coherent slabs seen in the Eastern belt may be remnants of sedimentary sources for high-grade blocks. This aligns with recent observations of homogeneous mean and maximum pressures of northern Franciscan eclogite blocks revealed by quartz-in-garnet barometry which suggest that they were coherently underplated and exhumed from similar structural levels (Cisneros et al., 2022).

## 7.2. Anomalous high-temperature serpentinite-mud matrix: remnants of diapirism?

The two serpentinite-rich samples from North Shell Beach and Goat Rock analyzed in this study had matching anomalously high temperatures of  $\sim 387$  °C. Their distinct thermal history and petrology indicate that they result from a different genetic process than the purely siliciclastic matrix mélanges. While conclusions based on only two samples are largely speculative in the absence of more detailed investigation, some observations are worth mentioning. Sample SB210726-1 was collected from a clastic serpentinite-selvage in close association with a  $\sim 60$  m garnet-amphibolite block (see Figure 12A-D in Wakabayashi, 2021b). Both the selvage of detrital serpentinite-mud and the garnet amphibolite block are in contact with  $\sim 200$  °C mud matrix mélange, in which they appear to be incorporated as a group. This perhaps represents an earlier matrix which originally enclosed the block. Sample GR210726-2 was from a more coherent detrital serpentinite-rich mélange body. Clear contact relationships with bounding units were not discerned in the field, but it appears to be contained within surrounding mud matrix mélange (see Figure 14 in Wakabayashi, 2015 for a geologic map. The unit in question is the northernmost serpentinite unit).

Wakabayashi (2012, 2015) has observed that many of the serpentinite mélange horizons of the Franciscan appear to be detrital in origin and has proposed that early exhumation of high-grade blocks was accommodated by serpentinite diapirs. These would be Franciscan equivalents to modern serpentinite mud volcanoes of the Marianas forearc that are known to carry high-grade blocks from depth (e.g. Fryer, 1999, 2000; Maekawa et al., 2008). However, unambiguous examples of preserved serpentinite diapirs that formed contemporaneously with Franciscan subduction remain elusive. One proposed diapir that may have sourced the serpentinite-rich olistostromes of the basal GVG has been reported (Jayko and Blake, 1986; Shervais et al., 2011). The massive 28 x 8 km serpentinite body at New Idria has also been suggested to be a deeply sourced diapir that accommodated exhumation of high-grade blocks (Tsujimori, 2007), but the timing of its structural development relative to Franciscan subduction processes remains unclear (e.g. Wakabayashi, 2015).

The high-T matrix of the two Franciscan serpentinite-mud samples suggests a deep source. Ultramafic clasts from Marianas serpentinite mud volcanoes cored during the IODP Expedition 366 drilling program experienced a maximum metamorphic temperature of 400 °C based on conversion of lizardite to antigorite (Debret et al., 2019) which is intriguingly close to

the temperature of Franciscan serpentinite-mud matrix obtained in this study (~387 °C). Further targeted investigation of detrital serpentinite exposures and their characterization by RSCM thermometry would elucidate whether this high-T thermal history generalizes across the Franciscan or is a local effect.

### *7.3. Further characterization of Franciscan sandstones and beyond*

The heterogenous RSCM spectra obtained for Franciscan sandstones is unsurprising as it is expected that different populations of CM grains sourced from the continental margin would have different thermal histories. Sand-sized grains and larger are carried from their source regions by traction flows at the base of a river. Thus, a more diverse assemblage of CM-containing grains is associated with the Franciscan sandstones, in contrast to the muds which acquire CM from suspension settling in the water column. Wakabayashi has claimed that the coherent sandstones likely represent turbidites, which are interfingered and interbedded with siliciclastic mélanges (e.g. Wakabayashi, 2015, 2021b). Such gradational contacts between sandstones and mélanges have been observed in the field (see Figure 10l in Wakabayashi, 2017). As mentioned in Section 6, isolated analysis of spectra comprising the lowest temperature population of the CM grains would be desired to obtain accurate maximum metamorphic temperatures for the sandstones. If Franciscan sandstones are observed to have temperatures comparable to those of bounding mélanges it would strengthen the argument that they are syndepositional turbidites that underwent subsequent subduction-accretion as a fixed unit.

The current study does not have the sampling resolution to attack this problem, but our RSCM-PLS method has proven to be a valuable thermometry technique that may be applied for further study. Analysis of more mélange bodies and sandstones at different localities, and more detailed sampling at each specific locality, has the potential to resolve detailed thermal histories for siliciclastic rocks across the Franciscan.

## **8. Conclusions**

A new RSCM thermometer using PLS regression was developed to investigate subduction mélanges in the Franciscan Complex. The results confirm a large difference in metamorphic grade between the mud matrix and high-grade blocks that lie within the matrix. Mélange matrix samples from North Shell Beach, Goat Rock, Mount Diablo, Sunol Regional

Wilderness, the Diablo Range, and San Simeon returned maximum metamorphic temperatures of 190 – 238 °C while commonly enclosing high-grade blocks that reached temperatures of ~300 – 630 °C. These matrix temperatures correspond to burial depths of only 13 – 20 km assuming a geothermal gradient of 10 – 15 °C for the Franciscan, and thus the matrix could not have reached the depths necessary for the entrainment of most high-grade blocks.

The mud matrix samples gave consistent Raman spectra and temperatures indicating that the enclosed CM grains have a similar thermal history. This is at odds with the subduction channel interpretation where a wider range of temperatures would be expected corresponding to *mélange* that upwelled from different depths. Furthermore, we suggest that chaotic mixing by Stokes settling through the flowing subduction channel cannot account for the size range of blocks observed in *mélanges*. Rather, we propose that the low temperature and uniform thermal history of mud matrix *mélanges* in the Franciscan is consistent with their deposition as submarine debris flows, where suspended mud acquired CM as it settled through the water column. The observed maximum metamorphic temperature in this study is thus an indicator of burial from subsequent subduction-accretion. In contrast, traction during the transport and deposition of Franciscan sandstones results in the inheritance of detrital CM grains with varied thermal histories as evidenced by their heterogeneous Raman spectra.

Analysis of two serpentinite-rich *mélange* samples obtained in this study from the North Shell Beach/Goat Rock region gave high maximum metamorphic temperatures of ~387 °C. These also shared a uniform thermal history, distinct from that of surrounding mud matrix *mélange*. One sample occurs in an isolated selvage associated with a large ~60 m garnet-amphibolite block with which it appears to share a genetic relationship. The anomalously high temperatures of these serpentinite-mud matrix *mélange* samples suggest a deep origin, and we speculate that they are sourced from diapirs as has been suggested for other detrital serpentinites across the Franciscan.

The RSCM-PLS approach used in this study is a promising method for the estimation of maximum metamorphic temperatures. The process of graphitization is especially useful for thermometry studies due to its insensitivity to pressure and irreversibility. Our use of PLS regression to analyze Raman spectra based on a calibration dataset with well-characterized metamorphic temperatures builds on previous RSCM thermometers in the elimination of curve fitting techniques that are prone to operator bias. Furthermore, rather than comparing various

discretionary parameter ratios, changes across the entire spectral window are considered when building the PLS model. Modified calibration datasets used in future studies should emphasize samples with well-constrained independent metamorphic temperatures as well as uniform thermal histories for CM grains.

### **Acknowledgements**

This work would not have been possible without the guidance of Mark Brandon who kept me in check throughout the entire process and never turned away a chance to discuss questions pertaining to tectonics, general geology, or anything under the sun. I also thank Jay Ague for taking the time to turn the petrographic microscope from a glorified kaleidoscope into a useful tool for my analytical repertoire. I am indebted to John Wakabayashi for his guidance during a field trip through the Franciscan in late July of 2021 which proved invaluable in formulating this project. That field trip, and subsequent research, were possible due to generous funding provided by the Karen L. Von Damm Undergraduate Research Fellowship in Earth & Planetary Sciences. Darrel Cowan, Keno Lünsdorf, and Sveva Corrado kindly provided samples that were used in this project. And finally, thank you to the Yale Earth & Planetary Sciences Department for an amazing four years.

### **References**

- Aalto, K.R., 1981, Multistage mélangé formation in the Franciscan Complex, northernmost California: *Geology*, v. 9, p. 602–607.
- Aalto, K. R., 1989, Franciscan complex olistostrome at Crescent City, northern California: *Sedimentology*, v. 36, no. 3, p. 471-495.
- Anelli, L., Gorza, M., Pieri, M. and Riva, M., 1994, Subsurface Well Data in the Northern Apennines (Italy): *Memorie della Società Geologica Italiana*, v. 48, 461-471.
- Barker, C.E. and Goldstein, R.H., 1990, Fluid-inclusion technique for determining maximum temperature in calcite and its comparison to the vitrinite reflectance geothermometer: *Geology*, v. 18, no. 10, p. 1003-1006.
- Baxter, E. F., 2003, Natural constraints on metamorphic reaction rates: *in* Vance, D., Mueller, W., Villa Igor, M., (Eds.), *Geochronology; linking the Isotopic Record with Petrology and textures*, Geological Society Special Publications, v. 220, Geological Society of

- London, p. 183 – 202.
- Berkland, J.O., Raymond, L.A., Kramer, J.C., Moores, E.M., and O'Day, M., 1972, What is Franciscan? *American Association of Petroleum Geologists Bulletin*, v. 56, p. 2295–2302.
- Beysac, O., Goffe, B., Chopin, C., and Rouzaud, J. N., 2002, Raman spectra of carbonaceous material in metasediments: a new geothermometer: *Journal of Metamorphic Geology*, v. 20, no. 9, p. 859-871.
- Blake, M. C., Jr., Jayko, A. S., McLaughlin, R. J., and Underwood, M. B., 1988, Metamorphic and tectonic evolution of the Franciscan Complex, northern California, *in* Ernst, W. G., ed., *Metamorphism and crustal evolution of the western United States (Rubey Volume VII)*: Englewood Cliffs, New Jersey, Prentice-Hall, p. 1035–1060.
- Blake, M.C., Jr., Howell, D.G., and Jayko, A.S., 1984, Tectonostratigraphic terranes of the San Francisco Bay Region, *in* Blake, M.C., Jr., ed., *Franciscan geology of Northern California*: Los Angeles, California, Pacific Section, Society of Economic Paleontologists and Mineralogists, v. 43, p. 5–22.
- Bostick, N. H., 1974, Phytoclasts as indicators of thermal metamorphism, Franciscan assemblage and Great Valley sequence, *in* Geological Society of America Special Paper 153, p. 1–17.
- Brown, K., and Westbrook, G., 1988, Mud diapirism and subcretion in the Barbados Ridge accretionary complex: the role of fluids in accretionary processes: *Tectonics*, v. 7, no. 3, p. 613-640.
- Cisneros, M., Behr, W. M., Platt, J. P., and Anczkiewicz, R., 2022, Quartz-in-garnet barometry constraints on formation pressures of eclogites from the Franciscan Complex, California: *Contributions to Mineralogy and Petrology*, v. 177, no. 1, p. 1-23.
- Claussmann, B., Bailleul, J., Chanier, F., Mahieux, G., Caron, V., McArthur, A. D., Chaptal, C., Morgans, H. E., and Vendeville, B. C., 2022, Shelf-derived mass-transport deposits: origin and significance in the stratigraphic development of trench-slope basins: *New Zealand Journal of Geology and Geophysics*, v. 65, no. 1, p. 17-52.
- Coleman, R., and Lanphere, M. A., 1971, Distribution and age of high-grade blueschists, associated eclogites, and amphibolites from Oregon and California: *Geological Society of America Bulletin*, v. 82, no. 9, p. 2397-2412.
- Coleman, R.G., 2000, Prospecting for ophiolites along the California continental margin, *in*

- Dilek, Y.D., Moores, E. M., Elthon, D., and Nicolas, A., eds., Ophiolites and oceanic crust: New insights from field studies and the ocean drilling program: Boulder, Colorado, Geological Society of America Special Paper 349, p. 351–364.
- Cooper, F. J., Platt, J. P., and Anczkiewicz, R., 2011, Constraints on early Franciscan subduction rates from 2-D thermal modeling: *Earth and Planetary Science Letters*, v. 312, no. 1-2, p. 69-79.
- Cowan, D., 1972, Petrology and structure of the Franciscan assemblage northwest of Pacheco Pass, California [Ph. D. thesis]: Stanford, Calif., Stanford Univ, v. 1974, p. 1623-1634.
- Cowan, D. S., 1978, Origin of blueschist-bearing chaotic rocks in the Franciscan Complex, San Simeon, California: *Geological Society of America Bulletin*, v. 89, no. 9, p. 1415-1423.
- Cowan, D. S., 1985, Structural styles in Mesozoic and Cenozoic mélanges in the western Cordillera of North America: *Geological Society of America Bulletin*, v. 96, no. 4, p. 451-462.
- Cowan, D. S., and Mansfield, C. F., 1970, Serpentinite flows on Joaquin Ridge, southern coast ranges, California: *Geological Society of America Bulletin*, v. 81, no. 9, p. 2615-2628.
- Cowan, D. S., and Page, B. M., 1975, Recycled Franciscan material in Franciscan mélange west of Paso Robles, California: *Geological Society of America Bulletin*, v. 86, no. 8, p. 1089-1095.
- Debret, B., Albers, E., Walter, B., Price, R., Barnes, J., Beunon, H., Facq, S., Gillikin, D. P., Mattielli, N., and Williams, H., 2019, Shallow forearc mantle dynamics and geochemistry: New insights from IODP Expedition 366: *Lithos*, v. 326, p. 230-245.
- Dickinson, W. R., 1966, Table Mountain serpentinite extrusion in California Coast ranges: *Geological Society of America Bulletin*, v. 77, no. 5, p. 451-472.
- Dickinson, W. R., 1970, Relations of andesites, granites, and derivative sandstones to arc-trench tectonics: *Reviews of Geophysics*, v. 8, no. 4, p. 813-860.
- Dickinson, W. R., Ojakangas, R. W., and Stewart, R. J., 1969, Burial metamorphism of the late Mesozoic Great Valley sequence, Cache Creek, California: *Geological Society of America Bulletin*, v. 80, no. 3, p. 519-526.
- Dodson, M. H., 1976, Kinetic processes and thermal history of slowly cooling solids: *Nature*, v. 259, p. 551 – 553.
- Dumitru, T. A., Ernst, W. G., Hourigan, J. K., and McLaughlin, R. J., 2015, Detrital zircon U–Pb

- reconnaissance of the Franciscan subduction complex in northwestern California: *International Geology Review*, v. 57, no. 5-8, p. 767-800.
- Erickson, R., 2011, Petrology of a Franciscan olistostrome with a massive sandstone matrix: The King Ridge Road mélangé at Cazadero, California: *Geological Society of America Special Papers*, v. 480, p. 171-188.
- Erickson, R. C., Mattinson, J., Dumitru, T., and Sharp, W., 2004, Petrology, isotope geochemistry, and geochronology of a multiply-metamorphosed granitoid exotic block in a Franciscan olistostrome mélangé: Cazadero, California: *Geological Society of America Abstracts with Programs*, v. 36, no. 4, p. 39.
- Ernst, W., 1993, Metamorphism of Franciscan tectonostratigraphic assemblage, Pacheco Pass area, east-central Diablo Range, California coast ranges: *Geological Society of America Bulletin*, v. 105, no. 5, p. 618-636.
- Ernst, W.G., and McLaughlin, R.J., 2012, Mineral parageneses, regional architecture, and tectonic evolution of Franciscan metagraywackes, Cape Mendocino-Garberville-Covelo 30' × 60' quadrangles, northwest California: *Tectonics*, v. 31, p. TC1001.
- Evarts, R. C., and Schiffman, P., 1983, Submarine hydrothermal metamorphism of the Del Puerto ophiolite, California: *American Journal of Science*, v. 283, no. 4, p. 289-340.
- Fryer, P., Wheat, C., and Mottl, M., 1999, Mariana blueschist mud volcanism: Implications for conditions within the subduction zone: *Geology*, v. 27, no. 2, p. 103-106.
- Fryer, P., Lockwood, J.P., Becker, N., Phipps, S., and Todd, C.S., 2000, Significance of serpentine mud volcanism in convergent margins, *in* Dilek, Y., Moores, E.M., Elthon, D., and Nicolas, A., eds., *Ophiolites and oceanic crust: New insights from field studies and the ocean drilling program*: Boulder, Colorado, Geological Society of America Special Paper 349, p. 35-51.
- Gerya, T. V., Stöckhert, B., and Perchuk, A. L., 2002, Exhumation of high-pressure metamorphic rocks in a subduction channel: A numerical simulation: *Tectonics*, v. 21, no. 6, p. 6-1-6-19.
- Grigull, S., Krohe, A., Moos, C., Wassmann, S., and Stöckhert, B., 2012, "Order from chaos": a field-based estimate on bulk rheology of tectonic mélanges formed in subduction zones: *Tectonophysics*, v. 568, p. 86-101.
- Hitz, B., and Wakabayashi, J., 2012, Unmetamorphosed sedimentary mélangé with high-pressure

- metamorphic blocks in a nascent forearc basin setting: *Tectonophysics*, v. 568, p. 124-134.
- Hopson, C.A., Mattinson, J.M., Pessagno, E.A., Jr., and Luyendyk, B.P., 2008, California Coast Range Ophiolite: Composite Middle and Late Jurassic oceanic lithosphere, in Wright, J.E., and Shervais, J.W., eds., *Ophiolites, arcs, and batholiths: A tribute to Cliff Hopson*: Geological Society of America Special Paper 483, p. 1–101.
- Hopson, C.A., Mattinson, J.M., and Pessagno, E.A., Jr., 1981, Coast Range Ophiolite, western California, in Ernst, W.G., ed., *Geotectonic development of California, Rubey Volume I*: Englewood Cliffs, New Jersey, Prentice-Hall, p. 418–510.
- Hsü, K. J., 1968, Principles of mélanges and their bearing on the Franciscan-Knoxville paradox: *Geological Society of America Bulletin*, v. 79, no. 8, p. 1063-1074.
- Jayko, A., and Blake Jr, M., 1986, Significance of Klamath rocks between the Franciscan Complex and Coast Range ophiolite, northern California: *Tectonics*, v. 5, no. 7, p. 1055-1071.
- Killner, M. H. M., Rohwedder, J. J. R., and Pasquini, C., 2011, A PLS regression model using NIR spectroscopy for on-line monitoring of the biodiesel production reaction: *Fuel*, v. 90, no. 11, p. 3268-3273.
- Krohe, A., 2017, The Franciscan Complex (California, USA) – The model case for return-flow in a subduction channel put to the test: *Gondwana Research*, v. 45, p. 282-307.
- Lahfid, A., Beyssac, O., Deville, E., Negro, F., Chopin, C., and Goffe, B., 2010, Evolution of the Raman spectrum of carbonaceous material in low-grade metasediments of the Glarus Alps (Switzerland): *Terra Nova*, v. 22, no. 5, p. 354-360.
- Lunsdorf, N. K., Dunkl, I., Schmidt, B. C., Rantitsch, G., and von Eynatten, H., 2017, Towards a Higher Comparability of Geothermometric Data Obtained by Raman Spectroscopy of Carbonaceous Material. Part 2: A Revised Geothermometer: *Geostandards and Geoanalytical Research*, v. 41, no. 4, p. 593-612.
- Lunsdorf, N. K., and Lunsdorf, J. O., 2016, Evaluating Raman spectra of carbonaceous matter by automated, iterative curve-fitting: *International Journal of Coal Geology*, v. 160, p. 51-62.
- Maekawa, H., Yokose, H., Fryer, P., Sato, H., and Yoshida, S., 2008, Geological expedition of the serpentinite seamounts in the Mariana forearc: Yokosuka Cruise report YK-08-08

- Leg 1-1: Japan Agency for Marine-Earth Science Technology.
- Mazet, V., Carteret, C., Brie, D., Idier, J., and Humbert, B., 2005, Background removal from spectra by designing and minimising a non-quadratic cost function: *Chemometrics and Intelligent Laboratory Systems*, v. 76, no. 2, p. 121-133.
- Mulcahy, S., Starnes, J., Coble, M., Day, H., and Vervoort, J., 2014, Early, prolonged and variable metamorphism of exotic blocks in the Franciscan subduction complex, *in* *Proceedings Geological Society of America Abstracts with Programs*, Volume 46, p. 445.
- Mulcahy, S. R., Starnes, J. K., Day, H. W., Coble, M. A., and Vervoort, J. D., 2018, Early onset of Franciscan subduction: *Tectonics*, v. 37, no. 5, p. 1194-1209.
- Nakamizo, M., Honda, H., and Inagaki, M., 1978, Raman-spectra of ground natural graphite: *Carbon*, v. 16, no. 4, p. 281-283.
- Orange, D. L., 1990, Criteria helpful in recognizing shear-zone and diapiric mélanges: Examples from the Hoh accretionary complex, Olympic Peninsula, Washington: *Geological Society of America Bulletin*, v. 102, no. 7, p. 935-951.
- Page, F., Armstrong, L. S., Essene, E. J., and Mukasa, S. B., 2007, Prograde and retrograde history of the Junction School eclogite, California, and an evaluation of garnet–phengite–clinopyroxene thermobarometry: *Contributions to Mineralogy and Petrology*, v. 153, no. 5, p. 533-555.
- Platt, J., 1975, Metamorphic and deformational processes in the Franciscan Complex, California: Some insights from the Catalina Schist terrane: *Geological Society of America Bulletin*, v. 86, no. 10, p. 1337-1347.
- Platt, J. P., 2015, Origin of Franciscan blueschist-bearing mélange at San Simeon, central California coast: *International Geology Review*, v. 57, no. 5-8, p. 843-853.
- Rahl, J. M., Anderson, K. M., Brandon, M. T., and Fassoulas, C., 2005, Raman spectroscopic carbonaceous material thermometry of low-grade metamorphic rocks: Calibration and application to tectonic exhumation in Crete, Greece: *Earth and Planetary Science Letters*, v. 240, no. 2, p. 339-354.
- Ring, U., and Brandon, M. T., 1994, Kinematic data for the Coast Range fault and implications for exhumation of the Franciscan subduction complex: *Geology*, v. 22, no. 8, p. 735-738.
- Ring, U., and Brandon, M. T., 1999, Ductile deformation and mass loss in the Franciscan subduction complex: implications for exhumation processes in accretionary wedges:

- Geological Society, London, Special Publications, v. 154, no. 1, p. 55-86.
- Rutte, D., Garber, J., Kylander-Clark, A., and Renne, P. R., 2020, An exhumation pulse from the nascent Franciscan subduction zone (California, USA): *Tectonics*, v. 39, no. 10, p. e2020TC006305.
- Sengör, A.M.C., 2003, The repeated discovery of mélanges and its implications for the possibility and role of objective scientific evidence in the scientific enterprise, *in* Dilek, Y., and Newcomb, S., eds., *Ophiolite concept and the evolution of geologic thought: Geological Society of America Special Paper 373*, p. 385–446.
- Shervais, J.W., Choi, S.H., Sharp, W.D., Ross, J., Zoglman-Schuman, M., and Mukasa, S.B., 2011, Serpentinite matrix mélange: Implications for mixed provenance for mélange formation, *in* Wakabayashi, J., and Dilek, Y., eds., *Mélanges: Processes of formation and societal significance: Geological Society of America Special Paper 480*, p. 1–30.
- Shreve, R. L., and Cloos, M., 1986, Dynamics of sediment subduction, melange formation, and prism accretion: *Journal of Geophysical Research: Solid Earth*, v. 91, no. B10, p. 10229-10245.
- Silver, E. A., and Beutner, E. C., 1980, Melanges: *Geology*, v. 8, no. 1, p. 32-34.
- Tsujimori, T., Liou, J.G., and Coleman, R.G., 2007, Finding of high-grade tectonic blocks from the New Idria serpentinite body, Diablo Range, California: Petrologic constraints on the tectonic evolution of an active serpentinite diapir, *in* Cloos, M., Carlson, W.D., Gilbert, M.C., Liou, J.G., and Sorensen, S.S., eds., *Convergent margin terranes and associated regions: A tribute to W.G. Ernst: Geological Society of America Special Paper 419*, p. 67–80.
- Tsujimori, T., Matsumoto, K., Wakabayashi, J., and Liou, J., 2006, Franciscan eclogite revisited: Reevaluation of the P–T evolution of tectonic blocks from Tiburon Peninsula, California, USA: *Mineralogy and Petrology*, v. 88, no. 1, p. 243-267.
- Tuinstra, F., and Koenig, J. L., 1970, Raman Spectrum of Graphite: *Journal of Chemical Physics*, v. 53, no. 3, p. 1126-1130.
- Ukar, E., 2012, Tectonic significance of low-temperature blueschist blocks in the Franciscan mélange at San Simeon, California: *Tectonophysics*, v. 568, p. 154-169.
- Ukar, E., and Cloos, M., 2014, Low-temperature blueschist-facies mafic blocks in the Franciscan mélange, San Simeon, California: Field relations, petrology, and counterclockwise P-T

- paths: Geological Society of America Bulletin, v. 126, no. 5-6, p. 831-856.
- Verdoya, M., Gola, G., and El Jbeily, E., 2019, Conductive heat flow pattern of the central-northern Apennines, Italy: International Journal of Terrestrial Heat Flow and Applied Geothermics, v. 2, no. 1, p. 37-45.
- Wakabayashi, J., 2011, Mélanges of the Franciscan Complex, California: Diverse structural settings, evidence for sedimentary mixing, and their connection to subduction processes, *in* Wakabayashi, J., and Dilek, Y., eds., Mélanges: Processes of formation and societal significance: Geological Society of America Special Paper 480, p. 117–141.
- Wakabayashi, J., 2015, Anatomy of a subduction complex: Architecture of the Franciscan Complex, California, at multiple length and time scales: International Geology Review, v. 57, p. 669–746.
- Wakabayashi, J., 2017, Structural context and variation of ocean plate stratigraphy, Franciscan Complex, California: Insight into mélange origins and subduction-accretion processes: Progress in Earth and Planetary Science, v. 4, no. 1, p. 1-23.
- Wakabayashi, J., 2021, Field and petrographic reconnaissance of Franciscan complex rocks of Mount Diablo, California: Imbricated ocean floor stratigraphy with a roof exhumation fault system, *in* Sullivan, R., Sloan, D., Unruh, J.R., and Schwartz, D.P., eds., Regional Geology of Mount Diablo, California: Its Tectonic Evolution on the North America Plate Boundary: Geological Society of America Memoir 217, p. 155–178.
- Wakabayashi, J., 2021b, Subduction and exhumation slip accommodation at depths of 10–80 km inferred from field geology of exhumed rocks: Evidence for temporal-spatial localization of slip, *in* Wakabayashi, J., and Dilek, Y., eds., Plate Tectonics, Ophiolites, and Societal Significance of Geology: A Celebration of the Career of Eldridge Moores: Geological Society of America Special Paper 552, p. 257–296.
- Wold, S., Sjöström, M., and Eriksson, L., 2001, PLS-regression: a basic tool of chemometrics: Chemometrics and intelligent laboratory systems, v. 58, no. 2, p. 109-130.
- Wopenka, B., and Pasteris, J. D., 1993, Structural characterization of kerogens to granulite-facies graphite: applicability of Raman microprobe spectroscopy: American Mineralogist, v. 78, no. 5-6, p. 533-557.
- Zattin, M., Picotti, V. and Zuffa, G.G., 2002, Fission-track reconstruction of the front of the Northern Apennine thrust wedge and overlying Ligurian unit: American Journal of

Science, v. 302, no. 4, p. 346-379.

## Supplementary Information

Table S1. Franciscan Siliciclastic Raman Thermometry Sample Locations

Sample <sup>a</sup>	Latitude	Longitude
<i>Melange matrix</i>		
SB210726-1	38°25'19" N	123°06'51" W
SB210726-2	38°25'19" N	123°06'51" W
SB210729-1	38°25'37" N	123°06'59" W
SB210729-3	38°25'37" N	123°06'59" W
SB210729-6	38°25'37" N	123°06'59" W
GR210726-2	38°26'29" N	123°07'32" W
MD210727-1	37°52'30" N	121°55'43" W
SRW210728-1	37°30'25" N	121°47'50" W
SRW210728-2	37°30'25" N	121°47'50" W
DR-53	37°12'19" N	121°19'10" W
DR-161	37°12'19" N	121°19'10" W
75S-5	35°38'34" N	121°11'11" W
<i>Sandstones</i>		
SB210729-2	38°25'45" N	123°07'03" W
GR210726-1	38°26'26" N	123°07'27" W
MD210727-2	37°52'30" N	121°55'43" W
SRW210728-3	37°30'42" N	121°47'59" W
<i>Unknown block-matrix relationships</i>		
MD210727-3	37°53'20" N	121°54'34" W
SRW210728-4	37°31'27" N	121°48'09" W
SRW210728-5	37°31'30" N	121°48'15" W
SRW210728-6	37°31'31" N	121°48'14" W